Histol Histopathol (2025) 40: 369-380

Histology and Histopathology
From Cell Biology to Tissue Engineering

ORIGINAL ARTICLE Open Access

Role of acupuncture in improving the outcome of sepsis-induced lung injury

Peng Li[1], Fangfang Li[2], Si Chen[3], Qiulei Ma[3], Jie Wang[3], Bingquan Ma[3] and Jin Xu[1]

[1]The Key Laboratory of Biomedical Information Engineering of Ministry of Education, Institute of Health and Rehabilitation Science, School of Life Science and Technology, Xi'an Jiaotong University, Xi'an, [2]Department of Dermatology, The Third Affiliated Hospital of Zhengzhou University, Zhengzhou University and [3]Department of Rehabilitation Medicine, The First Affiliated Hospital of Zhengzhou University, Zhengzhou, Henan, PR China

Summary. Objective. The purpose of this study was to investigate the effect of serum exosomes of mice after acupuncture (acu-exo) on acute lung injury (ALI) in sepsis *in vitro* and *in vivo*.

Methods. Serum exosomes (acu-exo) of normal mice were prepared after acupuncture. Lipopolysaccharide (LPS) was used to establish the model of ALI *in vivo* and *in vitro*. Immunohistochemistry, western blot, and immunofluorescence were used to evaluate the mechanism of acu-exo on ALI. P2X7 knockout mice and P2X7 siRNA were used to verify the mechanism.

Results. Compared with normal mice, serum exosomes were significantly increased in normal mice after acupuncture. The results showed that P2X7 was increased in the lung of septic mice as compared with the WT group. It was also found that the increase in NLRP3 and NF-κB was accompanied by the activation of P2X7. Increased P2X7 led to activation of the P2X7 receptor causing mitochondrial dysfunctions in lung tissue of septic mice. Knockout of P2X7 or silenced P2X7 markedly decreased NLRP3 and NF-κB and led to mitochondrial function recovery in lung tissue of sepsis. At the same time, acu-exo significantly restored the above changes in the lung tissue of septic mice.

Conclusions. Inhibition of P2X7 led to mitochondrial function recovery of lung tissue by inhibiting NLRP3 and NF-κB. At the same time, acu-exo could improve ALI by decreasing NLRP3 and NF-κB activation.

Key words: Exosomes, P2X7, Sepsis, Acute lung injury, NOD-like receptor thermal protein domain associated protein 3

Corresponding Author: Jin Xu, The Key Laboratory of Biomedical Information Engineering of Ministry of Education, Institute of Health and Rehabilitation Science, School of Life Science and Technology, Xi'an Jiaotong University, Xi'an, 710049, PR China. e-mail: xujinxjtu@163.com

www.hh.um.es. DOI: 10.14670/HH-18-781

Introduction

Sepsis refers to systemic inflammatory response syndrome (SIRS) caused by infection, which is a serious life-threatening disease with multiple organ dysfunction (Cecconi et al., 2018). In 2017, the World Health Organization (WHO) reported that there were nearly 30 million sepsis patients worldwide every year, and the mortality rate was as high as 50-70% (Prescott and Angus, 2018). Acute lung injury (ALI) is one of the main complications of sepsis, which seriously threatens life and health (Chen et al., 2022). There are many causes of ALI, including infection, vascular diseases, drug effects, shock, and radiation pneumonia. Although supportive care, a ventilator, and appropriate antibiotics in acute respiratory distress syndrome can alleviate the progress of the disease to some extent, the clinical mortality rate is still as high as 25% to 40% (Sinha et al., 2023). Therefore, it is very important to find an effective treatment to reduce morbidity and mortality.

Research showed that acupuncture has remarkable effects on inflammatory diseases. Acupuncture is an important part of Chinese traditional medicine, with obvious clinical effects and of simple operation (Sun et al., 2020). Inflammatory disease is an important indication for acupuncture clinical practice. WHO recommends that acupuncture can treat 26 inflammatory diseases such as scapulohumeral peri-arthritis and rheumatoid arthritis (Jiang et al., 2020). The anti-inflammatory mechanism of acupuncture is complex and closely related to nerve and humoral regulation (Jung et al., 2021). Recently, a randomized controlled trial has

Abbreviations. NF-κB, Nuclear factor-kappa B; P2X7, ATP-gated ion channels; ASC, apoptosis-associated speck-like protein; RAGE, advanced glycation end products receptors; MAPK, mitogen-activated protein kinase; TCM, Traditional Chinese Medicine; SOD, Superoxide Dismutase, MDA, Malondialdehyde; GSH-Px, Glutathione peroxidase; (TNF)-α, Tumor necrosis factor, (IL)-6, Interleukin-6; ELISA, enzyme-linked immunosorbent assay.

shown that electroacupuncture (EA) at "Zusanli" (ST36) and "Shangjuxu" (ST37) can reduce the inflammatory response in patients with sepsis by decreasing the level of Tumor necrosis factor (TNF)-α and Interleukin (IL)-1β in serum (Jiang et al., 2023). Research demonstrated that EA at ST3 attenuated the inflammatory response in rats by activating vagal anti-inflammatory mechanisms, protecting organ function, and improving survival after hemorrhagic shock (Liu et al., 2023). Acupuncture with conventional treatment can improve intestinal permeability in sepsis patients and facilitate the recovery of intestinal function (Yang et al., 2023).

Exosomes are vesicles with a lipid bilayer membrane structure, which are released into the extracellular environment after the cell membrane is fused with the multivesicular body (MVB) of eukaryotic cells (Kalluri and LeBleu, 2020). Exosomes can carry various signal molecules such as protein, lipid, DNA, miRNA, etc., and can direct these key substances to target cells, reflecting or treating diseases (Pegtel and Gould, 2019). Exosomes, as non-immunogenic nanovesicles, and their bilayer membrane structure, can protect their contents from the influence of serum protease and immune reactions during the cell transportation of the body, and maintain biological stability for a long time (Wang et al., 2021). Therefore, exosomes are expected to be a new way to treat sepsis. However, due to the small ratio of normal body secretion and exocrine secretion, the amount obtained is small.

In this study, EA was used to stimulate two Zusanli points (ST36) of septic mice, and we found that the content of serum exosomes was increased, which alleviated the oxidative stress response in the lung and suppressed inflammation. In conclusion, acupuncture treatment is inexpensive, safe, and easy to operate, providing a new direction for the treatment of sepsis patients and further inheriting and developing the Chinese medical tradition.

Materials and methods

Reagent

Fetal bovine serum (FBS), Phosphate-buffered saline (PBS), and Dulbecco's Modified Eagles medium (DMEM) were purchased from the American National Hyclone Company. Transit-X2 Transfection was purchased from the American Minas Company. The endotoxin-free plasmid extraction kit was purchased from the Qiagen Company in Germany. The bicinchoninic acid (BCA) protein quantitative assay kit was purchased from the Beijing Pulilai Company, and the Western blot kit was purchased from the Promega Company in the United States. LPS was purchased from the Sigma Company. Diamino polyethylene glycol was purchased from the Yarebio Company. All antibodies were purchased from the Cell Signaling Technology Company.

Animals

C57BL/6J, WT mice (ICR, male, 6 weeks, 16-18 g), P2X7 KO mice (ICR, male, *P2X7*$^{-/-}$, 6 weeks, 16-18 g) were obtained from the Cyagen Biosciences Inc. All animal operations were approved by the Research Council and Animal Care and Use Committee of Animal Center of Zhengzhou University (No.20220809112).

Acupuncture intervention and related parameters

Mice in the model and EA groups were intraperitoneally injected with LPS (12 mg/kg, 0.1 mL/10 g) to prepare septic mouse models. The experimental group was given acupuncture pretreatment before modeling, while the model group was not given acupuncture. In the EA group, both Zusanli points (ST36) of mice were pretreated with EA. The standard acupoints of mice were located at the Zusanli point according to the National acupoint standard. The Zusanli point is located at the posterolateral side of the knee joint of the hind limb and in the muscle groove about 3 mm below the small head of the fibula. Acupuncture was given at both Zusanli points 45 min before modeling. EA Parameters were a needling Depth of 3 mm, continuous waveform, frequency 10Hz, intensity 0.76 mA, time 15 min. In the process of EA pretreatment, the mice were fixed with a mouse fixator, as shown in Figure 1A, and the other groups of mice were grabbed and fixed in the same way.

Specific process of electroacupuncture in normal mice

Sixty C57BL/6J male mice were randomly divided into the control group (E0), EA 1-day normal mice (E1), EA 7-day normal mice (E7), EA 14-day normal mice (E14), and EA 21-day normal mice (E21), with 12 mice in each group.

All groups were fixed with a mouse fixator for 15 min, in which the normal mouse group (E0) had no EA intervention after 0 days of EA, and the intervention frequency of the normal mouse group (E1) after 1 day of EA was once for 1 day. The intervention frequency of EA in 7-day normal mice (E7) was once a day for 7 days. The frequency of EA for 14-day normal mice (E14) was once a day for 14 days. The intervention frequency of EA in 21-day normal mice (E21) was once a day for 21 days. In the control group, EA was not used to interfere with the Zusanli point but the fixator was used for 15 min.

Extract serum

After anesthetizing the mice with isoflurane, the skin behind the left and right ears of the mice was gently scratched with the left hand to expose the eyeballs, the mustache was trimmed to avoid hemolysis, the eyeballs were held with the right hand with sterile bending forceps, and the blood collection tube 2 mL tube was

quickly approached. The blood naturally drips into the tube, and the blood sample stood at room temperature for 2 hours and was then centrifuged in a low-temperature high-speed centrifuge 4°C, 3000g, 10min). About 400 μL of the extracted supernatant was put into an EP tube for preservation.

Separation and cracking of exosomes

The Exo Quick Precipitation method was used to extract serum exosomes, strictly following the instructions of the kit.

Exosome protein quantification by BCA

A 1:4 volume of RIPA protein lysate (RIPA protein buffer) to the Acu-exo sample size was added into the Acu-exo, mixed evenly, placed in an ice box, and incubated for 30 min until exosomes were completely lysed. Then, the content of Acu-exo protein was detected according to BCA kit instructions.

Establishment of the ALI mouse model

The ALI mouse model was established by intraperitoneal injection of LPS 10 mg/kg. The WT mice (control group) were given the same amount of saline in the same way. Mice were divided into the following groups: WT mice (control), WT + LPS (model), WT + LPS + Acu-exo (4 mg/kg), *P2X7*$^{-/-}$ + LPS, *P2X7*$^{-/-}$ + LPS + Acu-exo (4 mg/kg). After 24 hours of intervention, Acu-exo (4 mg/kg) was given to mice by gavage for 7 consecutive days.

In vitro model establishment

A549 cells were seeded in 6-well plates at a density of 1×10^6 cells/well for 24h. After that, the cells were divided into these groups: control, LPS (model, 50 mM), LPS + Acu-exo (50 μM), LPS + *P2X7* small interfering RNA (siRNA), LPS + *P2X7* siRNA + Acu-exo (50 μM). The cells were treated with Acu-exo (50 μM) for 24h, and 50 mM LPS were co-incubated for 24h, while the control group was challenged with an equal quantity of PBS. Cell supernatant and cells were collected for subsequent detection.

Cell transfection

A549 cells were inoculated in a 6-well plate with 5×10^4 cells per well, and cultured in DMEM containing 10% FBS in an incubator based on 37°C and 5% CO_2. When the cells grew to 50-70% confluence, various shRNA were transfected with the Translipid HL Transfection Reagent at a final concentration of 80 nmol/L according to the instructions of Translipid HL Transfection Reagent. Before transfection, the cells were cultured in 2 mL of serum-free DMEM medium for 2h, and after transfection for 6h, conventional DMEM medium containing 10% FBS was substituted for further culture. Six hours after transfection, the expression of green fluorescent protein in A549 cells was observed under a fluorescence microscope. Ten low-power fields were randomly selected, and the transfection efficiency was evaluated by counting the percentage of transfected cells over the total number of cells. Western blot was used to evaluate the success of cell transfection. The siRNA targeted for P2X7 (antisense, 5′ [Phos] CUUUAACGUCGGCUUGGGCUC [dT] [dT]-3′, and sense, 5′ [Phos] GCCCAAGCCGACGUUAAAGUA [dT] [dT]-3′, both synthesized by Sigma-Aldrich Company, was designed based on the Thomas Tuschl protocol. Lyophilized single-stranded RNA oligonucleotides were resuspended in sterile RNase-free water (100 μM), denatured (heated at 95°C for 5 min), aligned, and slowly annealed with decreasing temperature, resulting in the formation of double-stranded siRNA at 50 μM.

Measurement of the wet-dry ratio of the lung (w/d)

At the end of the experiment, the right lung of the mice was removed. The trachea and esophagus were passively separated, the right lung lobe was obtained, and the wet weight was measured immediately. Subsequently, the lungs were dried at 60°C for 72 hours to remove all moisture, and then weighed and the wet/dry (w/d) weight ratio of the lungs was calculated.

ROS and MPO test

Ten mg of lung tissue was added 1:10 with normal saline, centrifuged at 12000 rpm for 10 min, and the supernatant was collected and detected by ROS and MPO commercial kits. The process strictly followed the instructions of the kits.

Biochemical measurement

The levels of Superoxide Dismutase (SOD), Malondialdehyde (MDA), and Glutathione peroxidase (GSH-Px) were detected by a commercial kit, and the method was carried out according to the instructions.

Cytokine measurement

The concentrations of IL-6, IL-1β, and TNF-α in serum, lung tissues, and cell supernatant were analyzed by enzyme-linked immunosorbent assay (ELISA) kits according to the manufacturer's instructions.

Hematoxylin-eosin (HE) staining

The lung was fixed in a 4% formalin solution, embedded in paraffin, cut into 4-μm thick sections, and placed on a glass slide for hematoxylin-eosin staining.

Cell viability and ROS assay

A549 cells were seeded in 96-well plates at a density

of 1×10^4 cells/well for 24h. After, the cells were treated with Acu-exo (50 μM) and 50 mM LPS and co-incubated for 48h, while the control group was challenged with an equal amount of PBS. One part was used for cell viability, the medium was removed and 200 μl 0.5 mg/ml MTT was added to each well for 4h. The supernatant was discarded and 150 μl DMSO was added to each well. The absorbance value of each well was determined at 490 nm with a microplate spectrophotometer. For the ROS assay, detection was carried out according to the instructions of the kit. The experiment was repeated three times.

Immunohistochemistry

Lung tissue slices were baked at 60°C for 1h, then paraffin was removed by xylene, dehydrated by gradient ethanol, and heated by sodium citrate buffer for antigen repair. After natural cooling to room temperature, it was cultured with 3% hydrogen peroxide for 10 min. Each section was sealed with 3% BSA at room temperature. After removing the blocking solution, the section was incubated with the primary antibody at 4°C overnight, the secondary antibody was incubated for 10 min, and washed with PBS three times, each time for 3 min, and the third antibody was incubated for 10 min, and washed with PBS for 3 min each time. Samples were stained with DAB and hematoxylin, dehydrated by gradient ethanol and xylene, dried, and sealed with neutral resin, and the expression of related proteins in lung tissue was observed under a light microscope.

Western blot analysis

Total protein was extracted from the lysate of lung tissue and cells, and the protein content was determined by the BCA method. SDS-PAGE electrophoresis was performed on protein samples and transferred to a PVDF membrane, 5% skimmed milk powder was added, sealed at room temperature for 2h, and incubated with the related equal primary antibodies respectively. The membrane was rinsed with TBST and then reacted with horseradish peroxidase-coupled secondary antibody. The membrane was rinsed with TBST and then developed with an enhanced chemiluminescence luminescent (ECL) reagent. The optical density of the main band was measured by grey-scale imaging software (UVP, UK) to calculate the expression level of the proteins in lung tissue.

Immunofluorescence

The levels of NLRP3 in A549 cells were evaluated by immunofluorescence. Briefly, cultured A549 were washed twice with PBS, fixed with 4% paraformaldehyde (PFA) for 30 min, and then permeabilized with 0.5% Triton X-100 in PBS for 5 min, and blocked with 5% BSA for 1 h. The cells were incubated with the primary antibody NLRP3 (1:500) overnight at 4ºC, washed three times with PBS, and incubated with goat anti-rabbit IgG (H+L) secondary antibody Alexa Fluor® 488 conjugate (1:500) for 1h. After washing three times with PBS, DAPI was performed at room temperature for 5 min. Fluorescence images were taken by fluorescence microscopy.

Statistical analysis

All data were expressed as mean ± standard deviation (SD) and analyzed by one-way analysis of variance (ANOVA) followed by Tukey's multiple comparison test using GraphPad Prism 5 (GraphPad Software, USA). A value of $p<0.05$ was considered statistically significant.

Results

Quantitative detection results of Acu-exo proteins

The extracted serum exosomes are shown in Fig. 1B. The total protein concentrations of Acu-exo extracted from normal mice (E0), EA for 1 day (E1), EA for 7 days (E7), EA for 14 days (E14), and EA for 21 days (E21) were quantified by BCA, being 14.218 mg/mL,

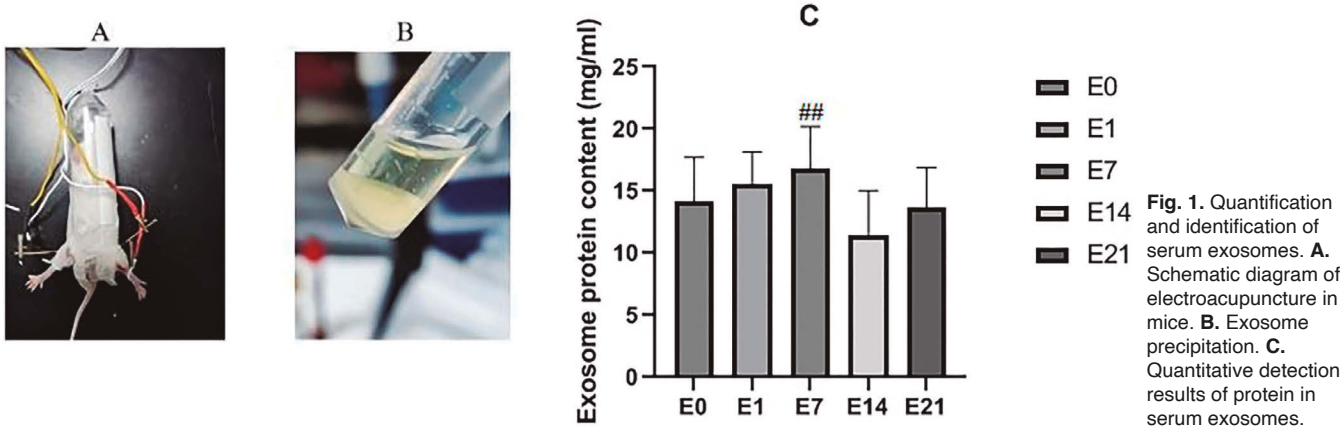

Fig. 1. Quantification and identification of serum exosomes. **A.** Schematic diagram of electroacupuncture in mice. **B.** Exosome precipitation. **C.** Quantitative detection results of protein in serum exosomes.

15.559 mg/mL, 16.794 mg/mL, 11.4221 mg/mL, and 13.695 mg/mL, respectively (Fig. 1C). In our previous pre-experiments, by infusing Acu-exo intraperitoneal reinfusion into septic mice, we found that exosomes on day 7 were most effective in improving survival in mice. Therefore, we chose E7-Acu-exo for the follow-up experiments.

Acu-exo alleviated w/d, ROS, and MPO in septic mice

As shown in Fig. 2A-C, the levels of w/d, ROS, and MPO were markedly increased in the model group than

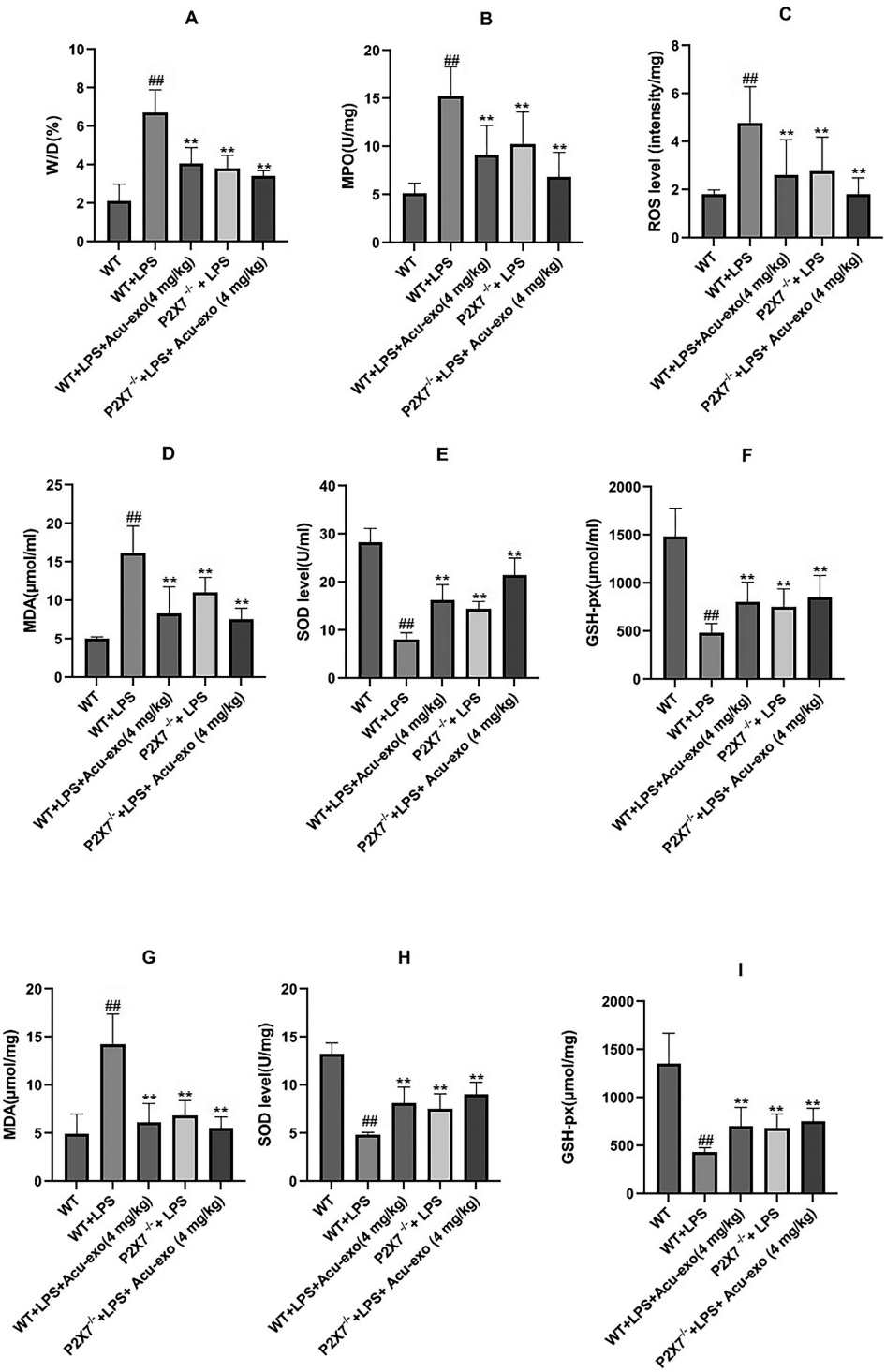

Fig. 2. Acu-exo significantly alleviated w/d, improved MPO, lung function indicators, oxidative stress indicators, and lung histopathology in septic mice. **A.** Acu-exo improved w/d (n=8). **B, C.** Acu-exo improved MPO and decreased ROS in the lung of septic mice (n=8). **D-F.** Acu-exo improved serum oxidative stress indicators, such as SOD, MDA, and GSH-Px in septic mice (n=8). **G-I.** Acu-exo increased the anti-oxidant effect in septic mice, increased concentrations of SOD, GSH-Px, and decreased MDA in the lung (n=8). All data are presented as mean ± SD. Compared with the control group: $^{\#\#}p<0.01$. Compared with the model group: $^{**}p<0.01$.

in the control group. Meanwhile, Acu-exo (4 mg/kg), markedly restored this change.

Acu-exo alleviated oxidative stress indicators, lung histopathology, and lung inflammation in mice

As shown in Fig. 2D-F, the levels of MDA in serum were increased, and SOD and GSH-px in serum were decreased compared with the control group, preliminarily showing sepsis-induced lung damage. Further, Acu-exo (4 mg/kg), *P2X7*$^{-/-}$ and *P2X7*$^{-/-}$ + Acu-exo (4 mg/kg) also reversed the sepsis-induced increase in MDA and decrease in SOD and GSH-px in serum, further demonstrating the improvement in lung oxidative

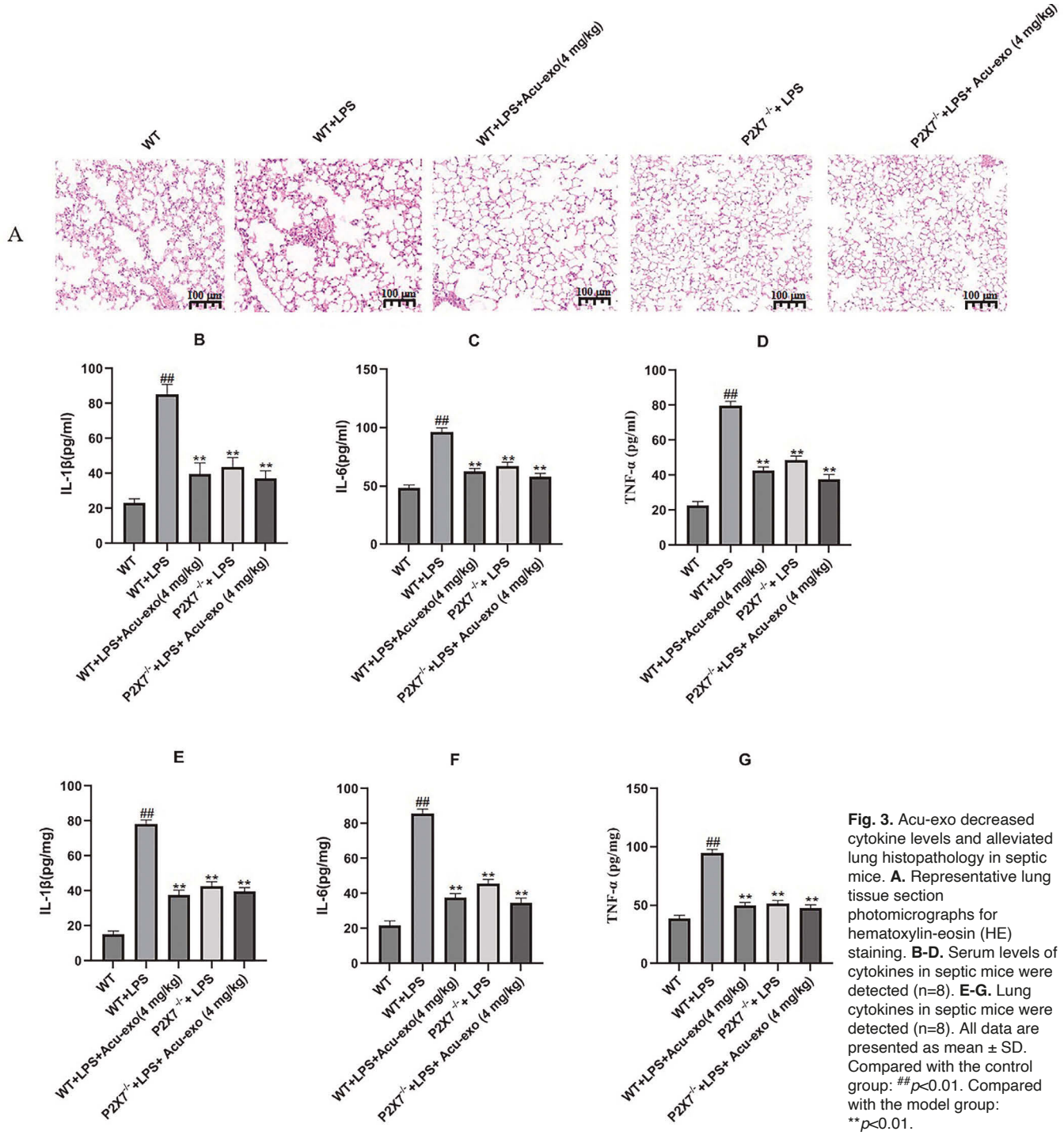

Fig. 3. Acu-exo decreased cytokine levels and alleviated lung histopathology in septic mice. **A.** Representative lung tissue section photomicrographs for hematoxylin-eosin (HE) staining. **B-D.** Serum levels of cytokines in septic mice were detected (n=8). **E-G.** Lung cytokines in septic mice were detected (n=8). All data are presented as mean ± SD. Compared with the control group: $^{\#\#}p<0.01$. Compared with the model group: $^{**}p<0.01$.

stress.

As shown in Fig. 2G-I, antioxidant indicators SOD and GSH-Px were decreased compared with the control group, whereas pro-oxidative indicators MDA increased in lungs. Acu-exo (4 mg/kg), *P2X7*$^{-/-}$ and *P2X7*$^{-/-}$ + Acu-exo (4 mg/kg) reversed sepsis-induced increased MDA and decreased SOD, GSH-Px in the lung, demonstrating that Acu-exo improves lung injury through anti-oxidant effects.

Pathological changes in the lung were evaluated by

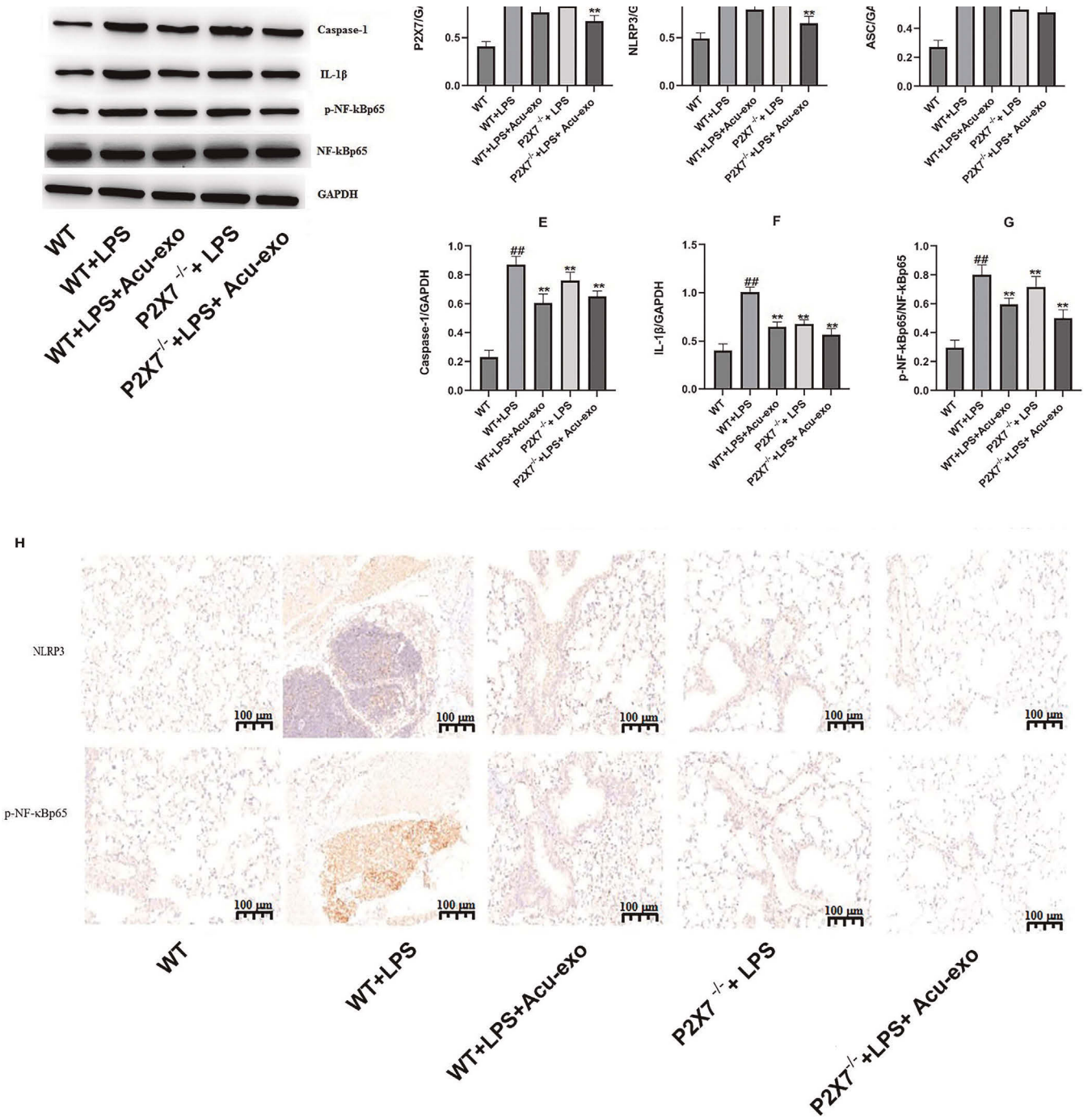

Fig. 4. Acu-exo inhibited P2X7-induced inflammation protein in septic mice. **A-G.** The levels of P2X7, NLRP3, p-NF-κB, ASC, caspase-1, IL-1β, and p-NF-κBp65 in the lungs of septic mice were detected by western blot analysis. Acu-exo inhibited the expression of these proteins in the lung of septic mice. **I.** Lung immunohistochemistry of NLRP3 and p-NF-κBp65 (n=3). All data are presented as mean ± SD. Compared with the control group: $^{\#\#}p<0.01$. Compared with the model group: $^{**}p<0.01$.

HE staining (Fig. 3A). Sepsis lung pathology exhibited by the mice in the model group showed diffuse congestion of the lung, local atrophy of the lung, widening of alveolar space, and infiltration of inflammatory cells. However, Acu-exo (4 mg/kg), *P2X7*$^{-/-}$, and *P2X7*$^{-/-}$ + Acu-exo (4 mg/kg) markedly restored the above changes in the lung.

In order to evaluate inflammatory reaction, cytokines (TNF-α, IL-1β, and IL-6) were detected. As expected, the levels of these inflammatory cytokines were increased in serum (Fig. 3B-D) and lung (Fig. 3E-G) in septic mice compared with the control group, showing that inflammation plays an important role in sepsis-induced lung injury. Acu-exo (4 mg/kg), *P2X7*$^{-/-}$ and *P2X7*$^{-/-}$ + Acu-exo (4 mg/kg) treatment significantly decreased these elevations in serum and lung, indicating that Acu-exo alleviated sepsis-induced lung injury by inhibiting the inflammatory response.

Acu-exo inhibited P2X7-induced inflammation protein in septic mice

As shown in Fig. 4A-G, compared with the control group, the levels of P2X7, NLRP3, NF-κBp65, apoptosis-associated speck-like protein (ASC), caspase-1, IL-1β, and p-NF-κBp65 were increased, Acu-exo (4 mg/kg), *P2X7*$^{-/-}$ and *P2X7*$^{-/-}$ + Acu-exo (4 mg/kg) significantly restored the changes in these proteins in septic mice. In immunohistochemistry experiments (Fig. 4I), as expected, Acu-exo (4 mg/kg), *P2X7*$^{-/-}$ and *P2X7*$^{-/-}$ + Acu-exo (4 mg/kg) treatment significantly decreased the levels of NLRP3 and p-NF-κBp65 in septic mice. In summary, the P2X7-NLRP3 signaling pathway plays a major role in sepsis-induced lung injury.

Acu-exo improved the LPS-induced A549-cell inflammatory reaction

We used LPS-stimulated A549 cells to detect the cell viability and anti-inflammatory effects of Acu-exo. As shown in Fig. 5A-D, Acu-exo showed no toxicity up to 100 μM in A549 cells. To determine the concentrations of LPS for modeling, LPS (12.5-100 mM) dose-dependently decreased A549 cell viability. Therefore, we choose 50 mM LPS for the A549-cell model concentration. LPS incubation significantly reduced A549-cell viability and increased ROS levels, while those were reversed by Acu-exo, *P2X7* siRNA, and Acu-exo + *P2X7* siRNA treatment.

To determine whether the inflammatory response is present in LPS-induced A549 cells, we used an ELISA kit to detect cell supernatant inflammatory cytokines. As shown in Fig. 5E-G, LPS could induce cytokine release in the cell supernatant of A549 cells, which was reversed by Acu-exo, *P2X7* siRNA, and Acu-exo + *P2X7* siRNA treatment.

We further explored the mechanism of LPS-induced A549 cells and the effect of Acu-exo. With the gradual increase of LPS concentration, the levels of P2X7, NLRP3, p-NF-κB, ASC, caspase-1, and p-NF-κB were increased in A549 cells (Fig. 5H-N). In addition, the levels of P2X7, NLRP3, p-NF-κB, ASC, caspase-1, and p-NF-κB were increased by LPS in A549 cells and were restored by Acu-exo, *P2X7* siRNA, and Acu-exo + *P2X7* siRNA. In immunofluorescence experiments (Fig. 5O,P), as expected, Acu-exo, p2X7 siRNA, and Acu-exo + *P2X7* siRNA significantly decreased the levels of NLRP3 and p-NF-κBp65 in A549 cells.

Acu-exo alleviated inflammation of A549 cells induced by P2X7

In order to confirm that Acu-exo acts through P2X7, recombinant human P2X7 protein was used to induce A549 cells; P2X7 concentrations from 0.125 to 1 μg/mL in A549 cells increased the levels of NLRP3, p-NF-κB (Fig. 6A-C), a concentration of 1 μg/mL was chosen for further experiments. Further, we examined the content of inflammatory cytokines in the P2X7-induced A549 cell supernatant. As shown in Fig. 6D-F, cytokines were increased by P2X7 in the A549 cell, whereas the changes were decreased by Acu-exo. In addition, western blotting was used to detect related proteins. As shown in Fig. 6G-L, P2X7 increased the levels of NLRP3 and p-NF-κBP65. Acu-exo markedly restored these changes, also immunofluorescence results showed that Acu-exo decreased the levels of NLRP3 and p-NF-κBp65 (Fig. 6M,N).

Discussion

In sepsis, lung injury is one of the most common organ dysfunctions (Wang et al., 2021b). We found that exosome injection tended to improve survival in septic mice and was accompanied by a significant reduction in lung injury and a decrease in inflammatory cells and water content in lung tissue. Exosomes have shown many pharmacological activities; specifically, exosomes have exhibited inspiring anti-inflammatory activities. However, due to the low secretion of exosomes, it is difficult to obtain them. In this study, EA was used to increase the exosomes secreted by the body and obtain enough exosomes to treat disease. In the present study, we reported a potent ability of Acu-exo to alleviate lung injury in septic mice. Furthermore, Acu-exo suppressed the P2X7 pathway, resulting in the reduction of lung injury and inflammatory response. We also used LPS or P2X7-induced A549 cells for further research. The results showed that Acu-exo against LPS and P2X7 induced an inflammatory response in a P2X7-dependent manner. P2X7 knockdown was used to determine the mechanism of LPS-induced A549 cells. These results implied that P2X7 played an important role in sepsis-induced lung injuries. There is growing evidence showing that oxidative stress caused by ROS accumulation and reduced antioxidant enzyme activity plays a non-negligible role in the progression of sepsis as it leads to mitochondrial dysfunction and further

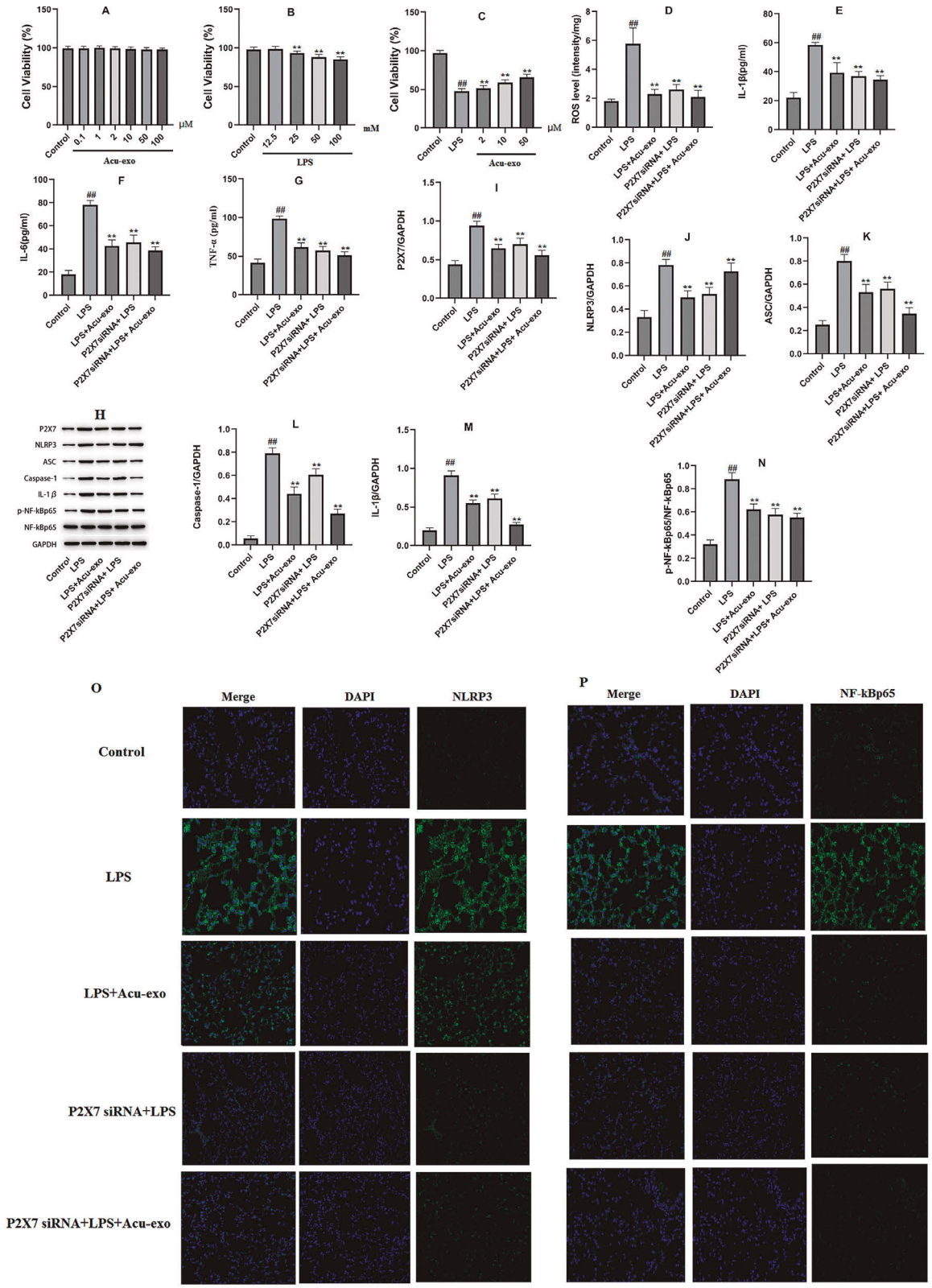

Fig. 5. Acu-exo improved LPS-induced A549-cell inflammatory reaction. **A.** Various concentrations of Acu-exo in A549 cells for 48h to investigate cytotoxicity (n=6. **B.** A549 cells were incubated with different concentrations of LPS for 48h to define the modeling concentration (n=6. **C, D.** Acu-exo improved LPS-induced A549-cell viability and decreased ROS (n=6), Acu-exo (2, 10, 50 μM) in A549 cells, followed by stimulation with 50 mM LPS for 48h. **E-G.** Acu-exo inhibited LPS-induced cytokines in A549 cells (n=6). **H-N.** LPS increased the P2X7-related protein in A549 cells and Acu-exo decreased the levels of P2X7-related protein in A549 cells. (O-P): Immunofluorescence results of NLRP3 and p-NF-κBp65 (n=3). All data are presented as mean ± SD. Compared with the control group: $^{\#\#}p<0.01$. Compared with the model group: $^{**}p<0.01$.

organ failure (Hajam et al., 2022).

In our study, LPS induced excessive levels of ROS, the accumulation of which triggers inflammation or cell death, which has been implicated in the pathogenesis of sepsis (Chen et al., 2023). Under physiological conditions, ROS production is counteracted by various cellular antioxidant enzymes to promote redox homeostasis. However, ROS accumulation could lead to an imbalance in favor of oxidants compared to antioxidant capacity. MDA, a marker of lipid peroxidation and antioxidant enzymes, including SOD and GSH-Px, reflects the extent of oxidative stress. Our study showed that the increased MDA and decreased SOD, GSH-Px in septic mice indicated increased ROS generation. Acu-exo treatment reduced ROS generation by decreasing MDA and restored antioxidant enzymes, including SOD and GSH-Px. At the same time, Acu-exo decreased ROS in mice and A549 cells.

MPO is a kind of heme enzyme, which is a specific marker of myeloid cells. It mainly exists in neutrophils and can catalyze chloride ions to generate hypochlorous acid and free radicals with oxidation ability, thus starting lipid peroxidation (Huang et al., 2020). Our results demonstrated that Acu-exo administration decreased MPO.

Despite updated diagnostic criteria, inflammation continues to be the primary pathogenesis and therapeutic target for sepsis, and excessive inflammatory responses are responsible for early deaths in patients with sepsis. Inflammatory cytokines, such as IL-1, IL-6, IL-18, and TNF-α, are critically involved in the pathogenesis of sepsis (Liu et al., 2022). IL-1β is synthesized by a variety of cell types, including macrophages, monocytes, and fibroblasts, and is an effective mediator of inflammation and immunity. Sepsis animal models have been demonstrated to increase the level of IL-1β (Xiong et al., 2020). IL-6 is another important inflammatory cytokine, and IL-6 mRNA in lungs with sepsis and serum IL-6 were demonstrated to be a candidate marker for sepsis (Zanders et al., 2022). TNF-α is a pro-inflammatory cytokine secreted from monocytes and macrophages that is functional in lipid metabolism, insulin resistance, and endothelial biology. TNF-α is involved in the pathogenesis of sepsis and if inhibited it will have significant therapeutic effects (Deng et al., 2022). Acu-exo markedly decreased the levels of cytokines in mice and A549 cells, showing that sepsis-induced lung injury can be relieved by inhibiting the inflammatory response.

The P2X7 receptor is the most special ion channel

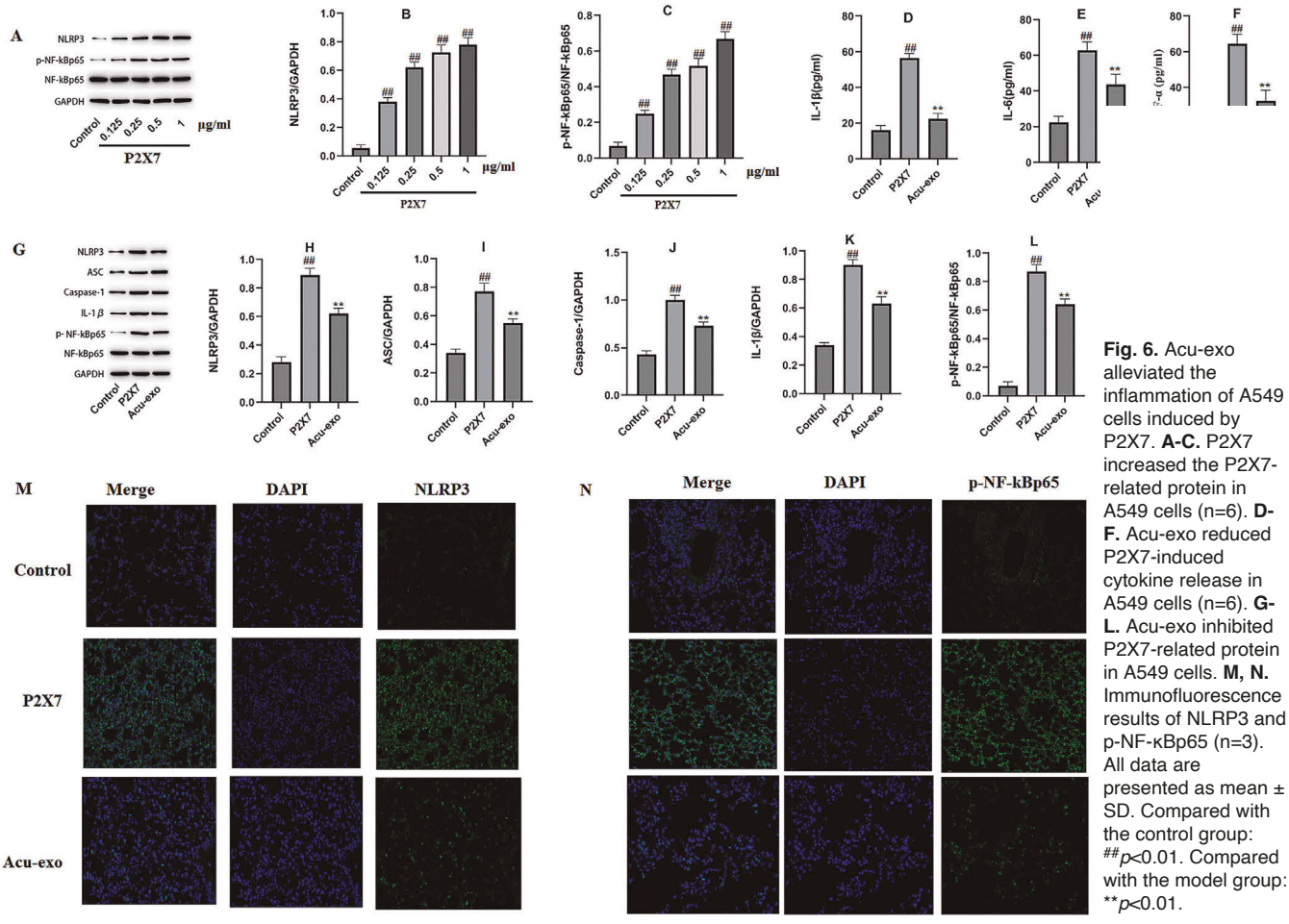

Fig. 6. Acu-exo alleviated the inflammation of A549 cells induced by P2X7. **A-C.** P2X7 increased the P2X7-related protein in A549 cells (n=6). **D-F.** Acu-exo reduced P2X7-induced cytokine release in A549 cells (n=6). **G-L.** Acu-exo inhibited P2X7-related protein in A549 cells. **M, N.** Immunofluorescence results of NLRP3 and p-NF-κBp65 (n=3). All data are presented as mean ± SD. Compared with the control group: $^{\#\#}p<0.01$. Compared with the model group: $^{**}p<0.01$.

receptor of the P2 family. It is mainly expressed in immune cells and also in many microglia, most bone marrow cells, granulocytes, monocytes/macrophages, B lymphocytes, lung, spinal cord, spleen, salivary glands intestinal tract, etc. It participates in many physiological functions such as cell signal transduction and cytokine secretion. In cell injury, mechanical stimulation, ischemia, or pathogen invasion induce intracellular to extracellular ATP release, and activation of the P2X7 receptor can be used as a danger signal to monitor early inflammation (Torres-Rodríguez et al., 2023). Many studies have shown that when tissues or cells are damaged, the concentration of extracellular ATP increases, which activates the P2X7 receptor, and then activates its downstream pathway NLRP3/Caspase-1, which further induces the maturation and release of IL-1β and initiates the inflammatory cascade reaction (Hayashi et al., 2023). Our study showed that Acu-exo markedly decreased the levels of P2X7, NLRP3/NF-κB both in mice and A549 cells, indicating that Acu-exo improves sepsis via downregulation of the P2X7 /NLRP3/ NF-κB signaling pathway.

To sum up, after acupuncture, the content of serum exosomes was increased, and sufficient exosomes could be obtained. Acu-exo significantly protects against lung inflammation induced by sepsis, and its mechanism may be related to the inhibition of the P2X7/NLRP3/NF-κB signaling pathway.

Limitations

For the first time, this study explains the increase in exocrine secretion and anti-inflammatory activity of acupuncture, however, there are two limitations: (1) This study was limited to the mouse level and did not involve humans or large animals; (2): This study only expounds the increase of exocrine volume by acupuncture but does not elaborate the specific mechanism of its increase.

Disclosure. The authors declare that they have no competing interests.

Data availability "statements". The datasets used and/or analyzed during the current study are available from the corresponding author upon reasonable request.

Funding. This research was supported by the Medical Science and Technology Project of Henan Province (LHGJ20210330).

References

Cecconi M., Evans L., Levy M. and Rhodes A. (2018). Sepsis and septic shock. Lancet 392, 75-87.

Chen R., Cao C., Liu H., Jiang W., Pan R., He H., Ding K. and Meng Q. (2022). Macrophage Sprouty4 deficiency diminishes sepsis-induced acute lung injury in mice. Redox Biol. 58, 102513.

Chen F., Chu C., Wang X., Yang C., Deng Y., Duan Z., Wang K., Liu B., Ji W. and Ding W. (2023). Hesperetin attenuates sepsis-induced intestinal barrier injury by regulating neutrophil extracellular trap formation via the ROS/autophagy signaling pathway. Food Funct. 14, 4213-4227.

Deng P., Tang N., Li L., Zou G., Xu Y. and Liu Z. (2022). Diagnostic value of combined detection of IL-1β, IL-6, and TNF-α for sepsis-induced cardiomyopathy. Med. Clin. 158, 413-417.

Hajam Y.A., Rani R., Ganie S.Y., Sheikh T.A., Javaid D., Qadri S.S., Pramodh S., Alsulimani A., Alkhanani M.F., Harakeh S., Hussain A., Haque S. and Reshi M.S. (2022). Oxidative stress in human pathology and aging: Molecular mechanisms and perspectives. Cells 11, 552.

Huang J., Yancey P.G., Tao H., Borja M.S., Smith L. E., Kon V., Davies S.S. and Linton M.F. (2020). Reactive dicarbonyl scavenging effectively reduces MPO-mediated oxidation of HDL and restores PON1 activity. Nutrients 12, 1937.

Hayashi K., Lesnak J. B., Plumb A. N., Rasmussen L. A. and Sluka K. A. (2023). P2X7-NLRP3-Caspase-1 signaling mediates activity-induced muscle pain in male but not female mice. Pain 164, 1860-1873.

Jang J.H., Yeom M.J., Ahn S., Oh J.Y., Ji S., Kim T.H. and Park H.J. (2020). Acupuncture inhibits neuroinflammation and gut microbial dysbiosis in a mouse model of Parkinson's disease. Brain Behav. Immun. 89, 641-655.

Jiang L.H., Li P.J., Wang Y.Q., Jiang M.L., Han X.Y., Bao Y.D., Deng X.L., Wu W.B. and Liu X.D. (2023). Anti-inflammatory effects of acupuncture in the treatment of chronic obstructive pulmonary disease. J. Integr. Med. 21, 518-527.

Jung J., Lee S.M., Lee M.J., Ryu J.S., Song J.H., Lee J.E., Kang G., Kwon O.S. and Park J.Y. (2021). Lipidomics reveals that acupuncture modulates the lipid metabolism and inflammatory interaction in a mouse model of depression. Brain Behav. Immun. 94, 424-436.

Kalluri R. and LeBleu V.S. (2020). The biology, function, and biomedical applications of exosomes. Science 367, eaau6977.

Liu D., Huang S.Y., Sun J.H., Zhang H.C., Cai Q.L., Gao C., Li L., Cao J., Xu F., Zhou Y., Guan C.X., Jin S.W., Deng J., Fang X.M., Jiang J.X. and Zeng L. (2022). Sepsis-induced immunosuppression: mechanisms, diagnosis and current treatment options. Mil. Med. Res. 9, 56.

Liu J., Zhu Q., Pan Y., Hao S., Wang Z., Cui C., Li J., Huang Y., Xia L., Xu T., Cheng J., Shen J. and Xia Y. (2023). Electroacupuncture alleviates intrauterine adhesion through regulating autophagy in rats. Mol. Hum. Reprod. 29, gaad037.

Pegtel D.M. and Gould, S.J. (2019). Exosomes. Annu. Rev. Biochem. 88, 487-514.

Prescott H.C. and Angus D.C. (2018). Enhancing recovery from sepsis: A Review. JAMA. 319, 62-75.

Sinha P., Meyer N.J. and Calfee C.S. (2023). Biological phenotyping in sepsis and acute respiratory distress syndrome. Annu. Rev. Med. 74, 457-471.

Sun N., Wang L.Q., Shao J.K., Zhang N., Zhou P., Fang S.N., Chen W., Yang J.W. and Liu C.Z. (2020). An expert consensus to standardize acupuncture treatment for knee osteoarthritis. Acupunct. Med. 38, 327-334.

Torres-Rodríguez O., Rivera-Escobales Y., Castillo-Ocampo Y., Velazquez B., Colón M. and Porter J.T. (2023). Purinergic P2X7 receptor-mediated inflammation precedes PTSD-related behaviors in rats. Brain Behav. Immun. 110, 107-118.

Wang C., Li Z., Liu Y. and Yuan L. (2021a). Exosomes in atherosclerosis: performers, bystanders, biomarkers, and therapeutic targets. Theranostics 11, 3996-4010.

Wang J.F., Wang Y.P., Xie J., Zhao Z.Z., Gupta S., Guo Y., Jia S.H.,

Parodo J., Marshall J.C. and Deng X.M. (2021b). Upregulated PD-L1 delays human neutrophil apoptosis and promotes lung injury in an experimental mouse model of sepsis. Blood 138, 806-810.

Xiong S., Hong Z., Huang L.S., Tsukasaki Y., Nepal S., Di A., Zhong M., Wu W., Ye Z., Gao X., Rao G.N., Mehta D., Rehman J. and Malik A.B. (2020). IL-1β suppression of VE-cadherin transcription underlies sepsis-induced inflammatory lung injury. J. Clin. Invest. 130, 3684-3698.

Yang L., Zhou D., Cao J., Shi F., Zeng J., Zhang S., Yan G., Chen Z., Chen B., Guo Y. and Lin X. (2023). Revealing the biological mechanism of acupuncture in alleviating excessive inflammatory responses and organ damage in sepsis: a systematic review. Front. Immunol. 14, 1242640.

Zanders L., Kny M., Hahn A., Schmidt S., Wundersitz S., Todiras M., Lahmann I., Bandyopadhyay A., Wollersheim T., Kaderali L., Luft F. C., Birchmeier C., Weber-Carstens S. and Fielitz J. (2022). Sepsis induces interleukin 6, gp130/JAK2/STAT3, and muscle wasting. J. Cachexia Sarcopenia Muscle 13, 713-727.

Accepted June 14, 2024